Proceedings of the EuroGNC 2013, 2nd CEAS Specialist Conference
on Guidance, Navigation & Control, Delft University of Technology,
Delft, The Netherlands, April 10-12, 2013

Aircraft Longitudinal Guidance Based on a Spatial Reference

H. Bouadi[1], D. Choukroun[2] and F. Mora-Camino[3]

Abstract In this study, instead of using time as the independent variable to describe the guidance dynamics of an aircraft, distance to land, which can be considered today to be available online with acceptable accuracy and availability, is adopted. A new representation of aircraft longitudinal guidance dynamics is developed according to this spatial variable. Then a nonlinear inverse control law based-on this new representation of guidance dynamics is established to make the aircraft follow accurately a vertical profile and a desired airspeed. The desired airspeed can be regulated to make the aircraft overfly different waypoints according to a planned time-table. Simulations results with different wind conditions for a transportation aircraft performing a descent approach for landing under this new guidance scheme are displayed.

1 Introduction

World air transportation traffic has known a sustained increase over the last decades leading to airspace near saturation in large areas of developed and emerging countries. For example, up to 27,000 flights cross European airspace every day while the number of passengers is expected to double by 2020. The available infrastructure of current ATM (Air Traffic Management) will no longer be able to stand this growing demand unless breakthrough improvements are made. In the air traffic management environment defined by SESAR and NextGen projects, two main objectives are targeted, strategic data link services for sharing of information and negotiation of planning constraints between ATC (Air Traffic Control) and the aircraft in order to ensure planning consistency and the use of the 4D aircraft trajectory information in the flight management system for ATC operations [1], [2] and [3]. This means that in addition to following the trajectory cleared by ATC, aircraft will progress in four dimensions, sharing accurate airborne predictions with the ground systems, and being able to meet time constraints at specific waypoints with high precision when the traffic density

[1]Hakim Bouadi
MAIAA, Air Transport Dept., ENAC, Toulouse, France, 31400, hakim.bouadi@enac.fr

[2] Daniel Choukroun
Space Systems Engineering, Faculty of Aerospace Engineering, Delft University of Technology, Delft, The Netherlands, 2629 HS, D.Choukroun@tudelft.nl

[3] Felix Mora-Camino
MAIAA, Air Transport Dept., ENAC, Toulouse, France, 31400, felix.mora@enac.fr

requires it [4], [5], [6] and [7]. This will allow better separation and sequencing of traffic flows while green climb/descent trajectories will be feasible in terminal areas.

Current civil aviation guidance systems operate with real time corrective actions to maintain the aircraft trajectory as close as possible to the planned trajectory or to follow timely ATC tactical demands based either on spatial or temporal considerations [8] and [9]. While wind remains one of the main causes of guidance errors [10], [11] and [12], these new solicitations by ATC are attended with relative efficiency by current airborne guidance systems. However, these guidance errors are detected for correction by navigation systems whose accuracy has known large improvements in the last decade with the hybridization of inertial units with satellite information. Nevertheless, until today vertical guidance remains problematic, [13] and [14], and corresponding covariance errors [15] are still large considering the time-based control laws which are applied by flight guidance systems [16].

In this paper, we consider the problem of designing a new longitudinal guidance control laws for an auto guidance system so that more accurate vertical tracking and overfly time are insured. There, instead of using time as the independent variable to describe the guidance dynamics of the aircraft, we adopt distance to land, which can be considered today to be available online with acceptable accuracy and availability. A new representation of aircraft vertical guidance dynamics is developed according to this spatial variable. Then a nonlinear inverse control law based-on this new proposed spatial representation of guidance dynamics is established to make the aircraft follow accurately a vertical profile and a desired airspeed [17] and [18]. The desired airspeed is then regulated to meet two main constraints related to the stall speed and the maximum operating speed and to make the aircraft overfly different waypoints according to a planned time-table.

Simulation experiments with different wind conditions are performed for a transportation aircraft performing a general descent approach for landing. It appears that with this new guidance scheme, vertical 2D+Time guidance can be achieved with accuracy.

2 Horizontal Distance to Land as an Independent Variable

The motion of an approach/descent transportation aircraft along a landing trajectory will be referenced with respect to a RRF (Runway Reference Frame) whose origin is located at the runway entrance as shown in Figure 1.

The vertical plane components of the inertial speed are such as:

$$\dot{x} = -V_{air}\cos\gamma_{air} + w_x \tag{1}$$

$$\dot{z} = V_{air}\sin\gamma_{air} + w_z \tag{2}$$

Then we can write:

$$V_{air} = \sqrt{(\dot{x} - w_x)^2 + (\dot{z} - w_z)^2} \tag{3}$$

$$\gamma_{air} = -arctg\left(\frac{\dot{z} - w_z}{\dot{x} - w_x}\right) \tag{4}$$

where x and z are the vertical plane coordinates of the aircraft centre of gravity in the RRF, V_{air} is the airspeed modulus, γ_{air} is the airspeed path angle, w_x and w_z are the wind components in the RRF.

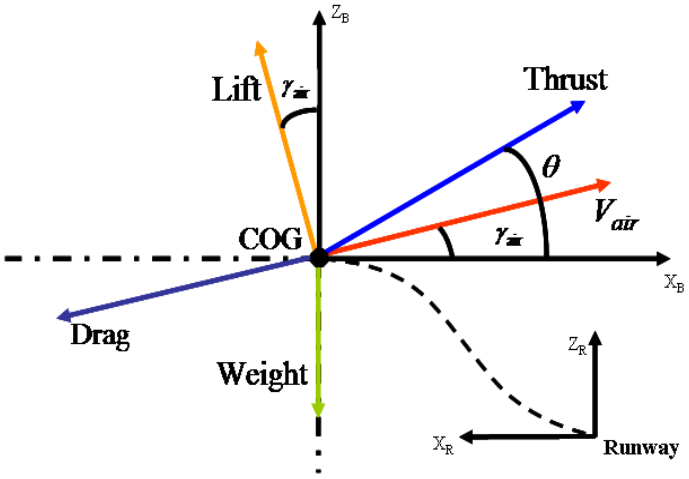

Fig. 1 Runway reference frame with aircraft forces and angles.

Supposing that during an approach/descent manoeuvre the distance-to-land time function $x(t)$ is invertible it is possible to express all the flight variables with respect to x and its derivatives instead of using time. Then for any time variable *v*, we have:

$$dv/dx = (dv/dt)(dt/dx) = \dot{v}/V_G \tag{5}$$

where the ground speed V_G at position *x* is given here by:

$$V_G = \dot{x} = -V_{air}\cos\gamma_{air} + w_x \tag{6}$$

Then the following notation is adopted for successive derivatives with respect to *x*:

$$\frac{d^k *}{dx^k} = *^{[k]} \tag{7}$$

3 Space Referenced Longitudinal Flight Dynamics

The aircraft longitudinal guidance dynamics can then be rewritten as:

$$z^{[1]} = \frac{dz}{dx} = \frac{dz}{dt}\frac{dt}{dx} = \frac{V_{air}\sin\gamma_{air} + w_z}{V_G} \tag{8}$$

$$\theta^{[1]} = q/V_G \tag{9}$$

$$V_{air}^{[1]} = \frac{1}{mV_G}\left[T\cos\alpha - D(z, V_{air}, \alpha) - mg\sin\gamma_{air} + m(\dot{w}_x\cos\gamma_{air} - \dot{w}_z\sin\gamma_{air})\right] \tag{10}$$

$$\gamma_{air}^{[1]} = \frac{1}{mV_{air}V_G}\left[T\sin\alpha + L(z, V_{air}, \alpha) - mg\cos\gamma_{air} - m(\dot{w}_x\sin\gamma_{air} + \dot{w}_z\cos\gamma_{air})\right] \tag{11}$$

where T, D and L are respectively the thrust, drag and lift forces. The lift and drag forces are classically given by:

$$L = \frac{1}{2}\rho(z)V_{air}^2 S\, C_L(\alpha) \tag{12}$$

$$D = \frac{1}{2}\rho(z)V_{air}^2 S\, C_D(\alpha) \tag{13}$$

where $\rho(z), S$, C_L and C_D represent the air density with respect to the altitude, the wing surface area, the lift and drag coefficients, respectively and where α denotes the angle of attack with here :

$$\alpha = \theta - \gamma_{air} \tag{14}$$

Assuming first order dynamics with time constant τ for the engines, we get between commanded thrust T_C and effective thrust T the following relation:

$$T^{[1]} = \frac{T_C - T}{\tau V_G} \tag{15}$$

then, with respect to $z^{[2]}$ we get:

$$z^{[2]} = \frac{1}{V_G^2}\left[\left(V_{air}^{[1]}\sin\gamma_{air} + V_{air}\gamma_{air}^{[1]}\cos\gamma_{air} + w_z^{[1]}\right)V_G - \left(V_{air}\sin\gamma_{air} + w_z\right)V_G^{[1]}\right] \tag{16}$$

Here q and T_C can be taken as independent control inputs to the above guidance dynamics while w_x and w_z are perturbation inputs. Equivalent control q is the result of pitch control on a very short time scale performed by the autopilot:

$$\dot{q} = M / I_y \tag{17}$$

where I_y denote the inertia moment and M is the pitch moment which can be approximated by affine expressions such as:

$$M = \frac{1}{2}\rho V_{air}^2 S\bar{c}\left(C_{m_0} + C_{m_\alpha}\alpha + C_{m_q}\frac{q\bar{c}}{2V_{air}} + C_{m_{\delta_e}}\delta_e\right) \tag{18}$$

with $\bar{c}$ and δ_e represent the mean chord line and the elevator deflection, respectively.

4 Longitudinal Trajectory Tracking Objectives

Here the considered guidance objectives consist for the aircraft first in following accurately a space-referenced vertical profile $z_d(x)$ defined in accordance with economic and environmental constraints, and second in matching a desired time table $t_d(x)$ during the approach manoeuver according to air traffic control directives. Of course, speed constraints must be satisfied during the manoeuver.

Trying to meet directly the second objective in presence of wind can lead to hazardous situations with respect to airspeed limits. So this objective is expressed through the on-line definition of a desired airspeed to be followed (it is supposed that online estimates of wind speed components are available). From a desired smooth time table $t_d(x)$, we get a desired ground speed $V_{G_d}(x)$:

$$V_{G_d}(x) = 1/(dt_d(x)/dx) \tag{19}$$

then, tacking into account an estimate of the longitudinal component of wind speed, a space-referenced desired airspeed $V_{air_d}(x)$ can be defined for low speeds by introducing a minimum margin with respect to the stall speed at the current desired level:

$$V_{air_d}(x) = \mathrm{Max}\left\{V_S(z_d(x)) + \Delta V_{\min}, V_{G_d}(x) - \hat{w}_x(x)\right\} \tag{20}$$

where V_S, $\Delta V_{\min}$ and $\hat{w}_x$ are respectively the stall speed, the minimum margin speed and the estimate of the horizontal wind speed. For high speeds, an airspeed less than the maximum operating speed at the current desired level:

$$V_{air_d}(x) = \mathrm{Min}\left\{V_{\mathrm{MO}}(z_d(x)), V_{G_d}(x) - \hat{w}_x(x)\right\} \tag{21}$$

where V_{MO} denotes the maximum operating speed.

In all other cases the desired airspeed is chosen such as:

$$V_{air_d}(x) = V_{G_d}(x) - \hat{w}_x(x) \tag{22}$$

5 Space-Based NLI Tracking Control

In this section the space-based nonlinear inverse control technique introduced in [18] to perform aircraft trajectory tracking is displayed. The relative degrees of output variables V_{air} and z can be determined from the following equations which are affine with respect to q and T_C :

$$V_{air}^{[2]} = \frac{1}{V_G^2}\left[A_V(z,\alpha,V_{air},T,W) + B_{V_q}(z,\alpha,V_{air},T,W)q + B_{V_T}(z,\alpha,V_{air},T,W)T_C\right] \tag{23}$$

$$z^{[3]} = \frac{1}{V_G^2}\left[A_z(z,\alpha,V_{air},T,W) + B_{z_q}(z,\alpha,V_{air},T,W)q + B_{z_T}(z,\alpha,V_{air},T,W)T_C\right] \tag{24}$$

where W represents the wind parameters w_x, w_z, $\dot{w}_x$, $\dot{w}_z$ and $\ddot{w}_x$ and $\ddot{w}_z$. The rather complex expressions of scalars A_V, B_{V_q}, B_{V_T} and A_z, B_{z_q}, B_{z_T} in (17) and (18) are detailed in [17].

The B_i terms are in general different from zero and the spatial relative degree of V_{air} and z are respectively $r_V = 1$ and $r_z = 2$. Then if V_{air} and z are chosen as tracked variables, there will be no internal dynamics to worry about. Now, since in standard flight conditions the control matrix B given by:

$$B = \begin{pmatrix} B_{z_q} & B_{z_T} \\ B_{V_q} & B_{V_T} \end{pmatrix} \tag{25}$$

is invertible, it is possible to perform a direct dynamic inversion to get effective trajectory tracking control laws, [22]. So we get:

$$\begin{pmatrix} q \\ T_C \end{pmatrix} = \begin{pmatrix} B_{z_q} & B_{z_T} \\ B_{V_q} & B_{V_T} \end{pmatrix}^{-1} \times \begin{pmatrix} V_G^2 D_z(x) - A_z \\ V_G^2 D_{V_{air}}(x) - A_V \end{pmatrix} \tag{26}$$

with:

$$D_z(x) = z_d^{[3]}(x) + k_{1z}\xi_z^{[2]}(x) + k_{2z}\xi_z^{[1]}(x) + k_{3z}\xi_z(x) \tag{27}$$

$$D_{V_{air}}(x) = V_{air_d}^{[2]}(x) + k_{1v}\xi_{V_{air}}^{[1]}(x) + k_{2v}\xi_{V_{air}}(x) \tag{28}$$

where with $\xi_z(x)$ and $\xi_{V_{air}}(x)$ are the tracking errors related to the desired altitude $z_d(x)$ and desired airspeed profile $V_{air_d}(x)$:

$$\xi_z(x) = z(x) - z_d(x) \tag{29}$$

$$\xi_{V_{air}}(x) = V_{air}(x) - V_{air_d}(x) \tag{30}$$

Then the tracking error variables follow the linear dynamics:

$$\xi_{V_{air}}^{[2]}(x) + k_{1v}\xi_{V_{air}}^{[1]}(x) + k_{2v}\xi_{V_{air}}(x) = 0 \tag{31}$$

$$\xi_z^{[3]}(x) + k_{1z}\xi_z^{[2]}(x) + k_{2z}\xi_z^{[1]}(x) + k_{3z}\xi_z(x) = 0 \tag{32}$$

where k_{1v}, k_{2v} , k_{1z} , k_{2z} and k_{3z} are real parameters which must be chosen such as the roots of $s^2 + k_{1v}s + k_{2v}$ and $s^3 + k_{1z}s^2 + k_{2z}s + k_{3z}$ produce adequate tracking error dynamics (stability and reduced oscillations). Here s denotes the Laplace variable.

Observe here that while the successive spatial derivatives of desired outputs $z_d(x)$ and $V_{air_d}(x)$ can be directly computed, the computation of the successive spatial derivatives of actual outputs $z(x)$ and $V_{air}(x)$ includes the wind parameters which have been replaced by their estimates.

Then we get a new two level control structure where the first layer corresponds to a fast control loop for the pitch rate (autopilot) and the thrust (autothrottle) on a time scale basis, while the second control layer, operating on a space scale basis, corresponds to a slow control loop of groundspeed and height.

6 Simulation Results

The proposed guidance approach is illustrated using the Research Civil Aircraft Model (RCAM) which has the characteristics of a wide body transportation aircraft, see again [23], with a maximum allowable landing mass of about 125 tons with a nominal landing speed of 68m/s. There, the control signals are submitted to rate limits and saturations as follows:

$$-15\frac{\pi}{180}\text{rad/s} \le \dot{\delta}_e \le 15\frac{\pi}{180}\text{rad/s} \tag{33}$$

$$-25\frac{\pi}{180}\text{rad} \le \delta_e \le 10\frac{\pi}{180}\text{rad} \tag{34}$$

$$-1.6\frac{\pi}{180}\text{rad/s} \le \dot{T}_C \le 1.6\frac{\pi}{180}\text{rad/s} \tag{35}$$

$$0.5\frac{\pi}{180}\text{rad} \le T_C \le 10\frac{\pi}{180}\text{rad} \tag{36}$$

While the minimum allowable speed is $1.23V_{stall}$ with $V_{stall} = 51.8\text{m/s}$ and the angle of attack is limited to the domain $\left[-11.5^\circ, 18^\circ\right]$ where $\alpha_{stall} = 18^\circ$.

6.1 Simulation Results in No-Wind Condition

In a no wind condition, Figure 2 displays altitude tracking performances resulting from a space NLI guidance scheme, while Figure 3 provides closer views of altitude and tracking performance during initial transients. Figure 4 displays airspeed tracking performances of a space NLI guidance scheme when the aircraft is initially late according to the planned time table. It appears clearly that the aircraft increases its airspeed to the maximum operating speed during 12000m until it catches up its delay.

Figures 5 and 6 display respectively the evolution of respectively the angle of attack, the flight path angle, the elevator deflection and the throttle setting during the whole manoeuvre. Since the angle of attack remains in a safe domain and the considered longitudinal inputs remain by far unsaturated this demonstrates the feasibility of the manoeuvre.

Figure 7 and Figure 8 show respectively airspeed and time tracking performances in two cases. The first one considers a delay situation for an aircraft according to a reference time table where the aircraft maintains its airspeed at V_{MO} until it compensates the initial delay. In the second situation the aircraft is initially in advance with respect to the planned time table and in this case the speed controller sets its airspeed to the minimum allowable speed until the time tracking error is eliminated.

6.2 Simulation Results in the Presence of Wind

Here a tailwind with a mean value of 12m/s has been considered. Figure 9 provides an example of realization of such wind.

Since in this study the problem of the online estimation of the wind components has not been tackled, it has been supposed merely that the wind estimator will be similar to a first order filter with a space constant equal to 28m in the other case (space NLI guidance). Then the filtered values of these wind components have been fed to the space NLI guidance control law.

Figure 10 and Figure 11 display altitude, airspeed and time tracking performances in the presence of the wind when the actual time table is late and in advance situations according to the reference time table, respectively.

7 Conclusion

In this communication a new longitudinal guidance scheme for transportation aircraft has been proposed.

The main objective here has been to improve the tracking accuracy performance of the guidance along a desired longitudinal trajectory referenced in a spatial frame. This has led to the development of a new representation of longitudinal flight dynamics where the independent variable is ground distance to a reference point. The nonlinear inverse control technique has been applied in this context so that tracking errors follow independent and asymptotically stable spatial dynamics around the desired trajectories. It has been shown also that a similar tracking objective expressed in the time frame cannot be equivalent when the desired airspeed changes as it is generally the case along climb and approach for landing.

Tracking performances obtained from this spatial NLI guidance scheme have been analyzed through a simulation study considering the descent maneuver of a transportation aircraft in wind and no wind conditions.

To get applicability this new guidance approach still should overcome important challenges related mainly with navigation and online wind estimation performances. Then an improved integration of on board flight path optimization functions including the consideration of neighbouring traffic and the guidance function will become possible.

References

[1] http://www.sesarju.eu/programme/highlights/i-4d-flight.

[2] De Smedt David, Thomas Putz, October 25-29, 2009, Flight Simulations Using Time Control With Different Levels of Flight Guidance, Orlando, Florida, USA, IEEE/AIAA 28th Digital Avionics Systems Conference, pp. 2.C.5-1-2.C.5-15.

[3] Teutsch Jurgen, Eric offman, 2004, Aircraft in the Future ATM System-Exploiting the 4D Aircraft Trajectory, USA, IEEE/AIAA 23rd Digital Avionics Systems Conference, pp. 3.B.2-1-3.B.2-21.

[4] Pappas. G, C. Tomlin, J. Lygeros, D. Godbole and S. Sastry, December, 1997, A Next Generation Architecture for Air Traffic Management Systems, San Diego, California, USA, IEEE Proceeding of the 36th Conference on Decision and Control, pp. 2405-2411.

[5] Bernd Korn, Alexander Kuenz, 2006, 4D FMS for Increasing Efficiency of TMA Operations, USA, IEEE/AIAA 25th Digital Avionics Systems Conference, pp. 1E4-1-1E4-8.

[6] Shih-Yih Young, Real-Time 4-D Trajectory Planning for RNP Flight Operations, IEEE Integrated communications, Navigation and Surveillance Conference, pp. 1-9, 2009.

[7] Mayte Cano, Pablo Sanchez-Escalonilla and Manuel. M. Dorado, 2007, Complexity Analysis in the Next Generation of Air Traffic Management System, Dallas, Texas, USA, IEEE/AIAA 26th Digital Avionics Systems Conference, pp. 3.D.4-1-3.D.4-9.

[8] Miele A, et al, 1986, Guidance Strategies for Near-Optimum Takeoff Performance in Wind Shear, Journal of Optimization Theory and Applications, Vol. 50, No. 1.

[9] Miele A, et al, 1986, Optimization and Gamma/Theta Guidance of Flight Trajectories in a Windshear, London, Presented at the 15th ICAS Congress.

[10] Miele A, et al, 1990, Optimal Trajectories and Guidance Trajectories for Aircraft Flight Through Windshears, Honolulu, Hawaii, Proceedings of the 29th Conference on Decision and Control, , pp. 737-746.

[11] Psiaki M.L. and R.F. Stengel, 1985, Analysis of Aircraft Control Strategies for Microburst Encounter, Journal of Guidance, Control, and Dynamics, Vol. 8, No. 5, pp. 553-559.

[12] Psiaki M.L. and K. Park, 1992, Thrust Laws for Microburst Wind Shear Penetration, Journal of Guidance, Control, and Dynamics, Vol. 15, No. 4.

[13] Singh S.N. and W.J. Rugh, 1972, Decoupling in a Class of Nonlinear Systems by State Feedback, ASME Journal of Dynamic Systems, Measurement, and Control, Series G, Vol. 94, pp. 323-329.

[14] Stengel, R.F, 1993, Toward Intelligent Flight Control, IEEE Trans. On Systems, Man, and Cybernetics, Vol. 23, No. 6, pp. 1699-1717.

[15] Sandeep S. Mulgund and Robert F. Stengel, January 1996, Optimal Nonlinear Estimation for Aircraft Flight Control in Wind Shear, Automatica, Vol.32, No. 1.

[16] Psiaki M.L, 1987, Control of Flight Through Microburst Wind Shear Using Deterministic Trajectory Optimization, Ph.D. Thesis, Department of Mechanical and Aerospace Engineering, Princeton University, Report No. 1787-T.

[17] Bouadi. H and F. Mora-Camino, May 17-18, 2012, Space-Based Nonlinear Dynamic Inversion Control for Aircraft Continuous Descent Approach, Madrid, Spain, IEEE Evolving and Adaptive Intelligent Systems Conference, pp. 164-169.

[18] Bouadi. H and F. Mora-Camino, August 13-16, 2012, Aircraft Trajectory Tracking by Nonlinear Spatial Inversion, Accepted in AIAA Guidance, Navigation and Control Conference, Minneapolis, Minnesota, USA.

[19] Etkin B, 1985, Dynamics of Atmospheric Flight, New York, John Wiley and Sons, Inc.

[20] Isidori A, Nonlinear Control Systems, Springer-Verlag, Berlin.

[21] Frost W, Bowles. R, 1984, Wind Shear Terms in the Equations of Aircraft Motion, Journal of Aircraft, Vol. 21, No.11, pp. 866-872.

[22] Campbell C. W, May 1984, A Spatial Model of Wind Shear and Turbulence for Flight Simulation, Tech. Rep. TP-2313, NASA George C. Marshall Space Flight Centre, Alabama 35812.

[23] Magni J-F. et al, Robust Flight Control, A Design Challenge, Springer-Verlag, London.

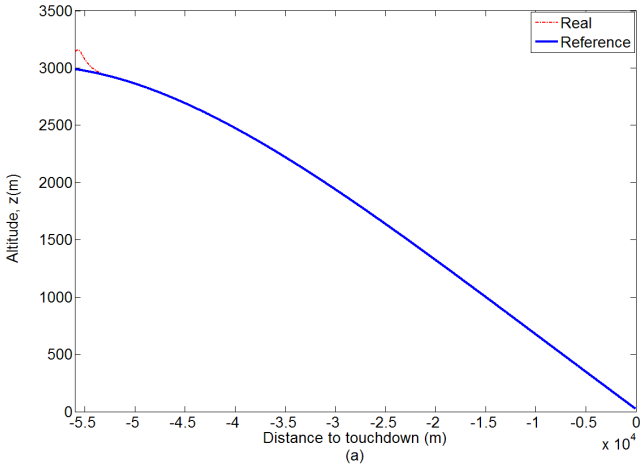

Fig. 2 Desired vertical tracking performance with space NLI (no wind).

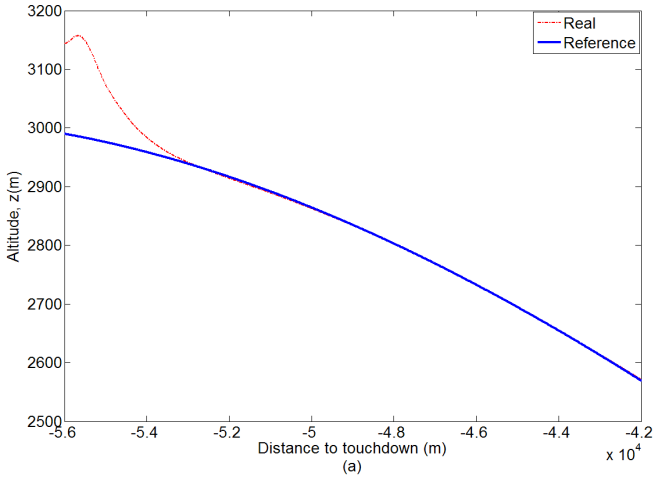

Fig. 3 Initial vertical tracking by space NLI (no wind).

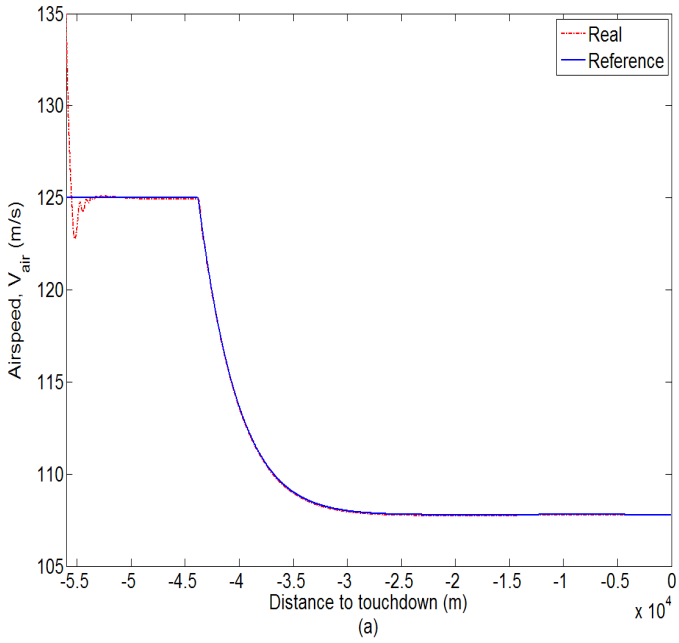

Fig. 4 Desired airspeed tracking performance (no wind).

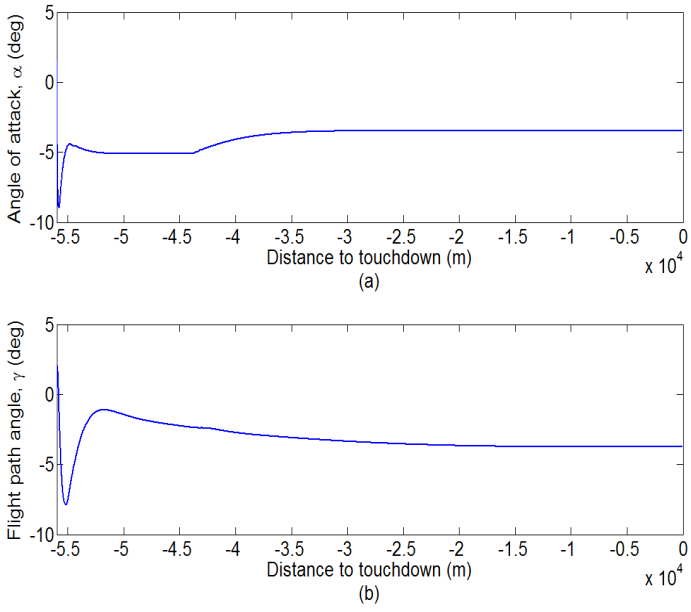

Fig. 5 Angle of attack and flight path angle with space NLI (no wind).

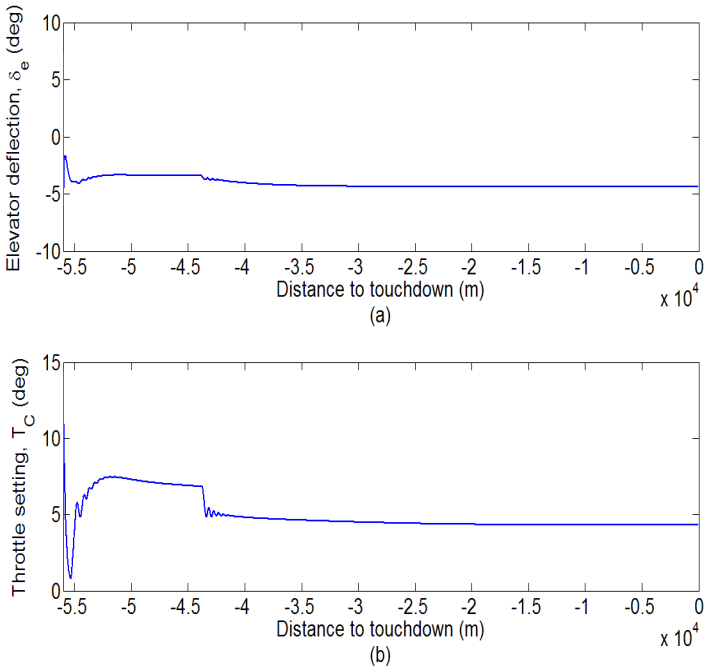

Fig. 6 Control inputs with space NLI (no wind).

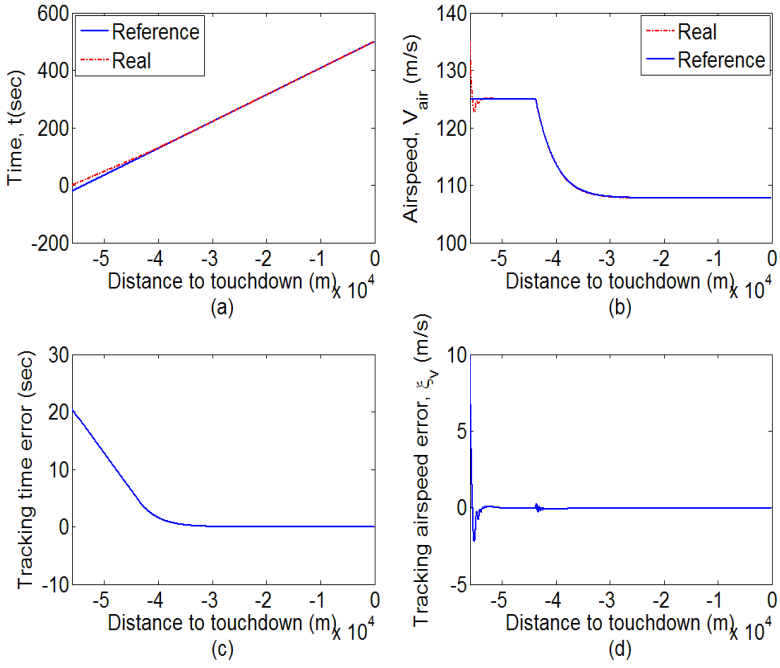

Fig. 7 Delayed initial situation and recover.

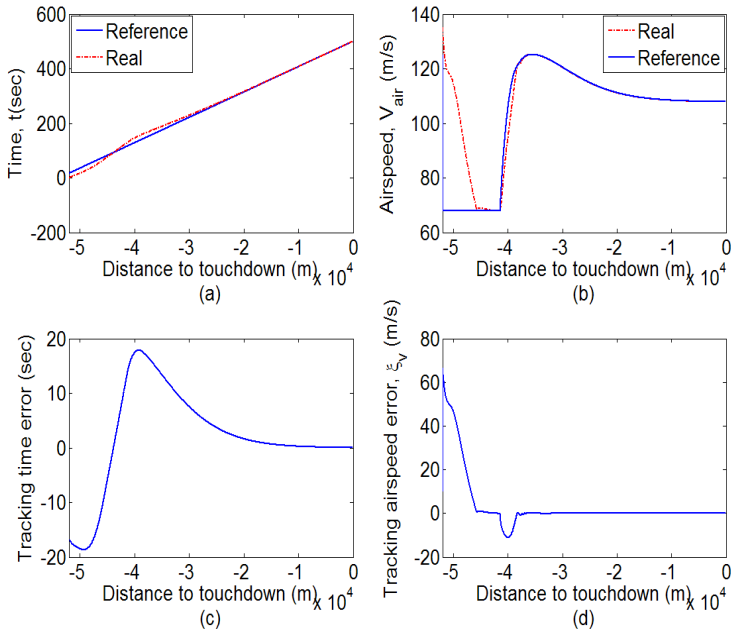

Fig. 8 Advanced initial situation and recover.

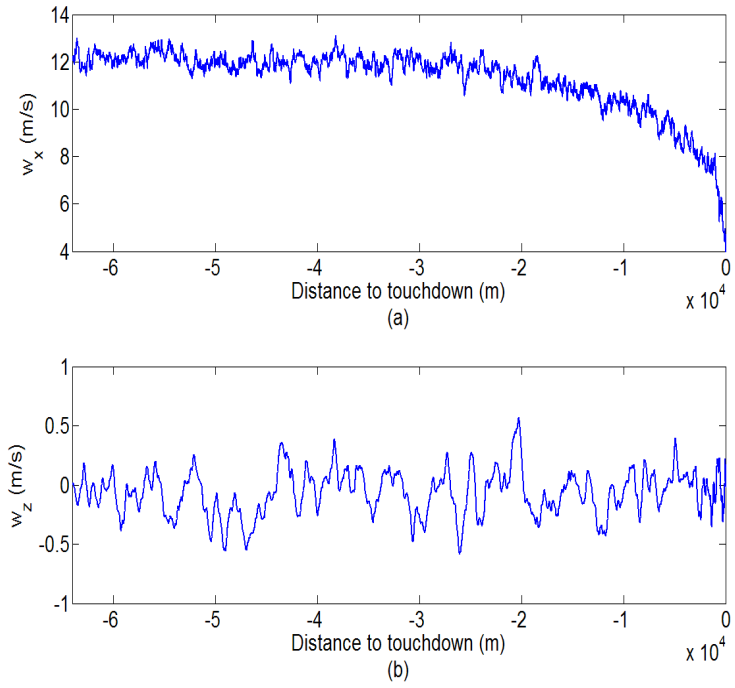

Fig. 9 Example of wind components space history.

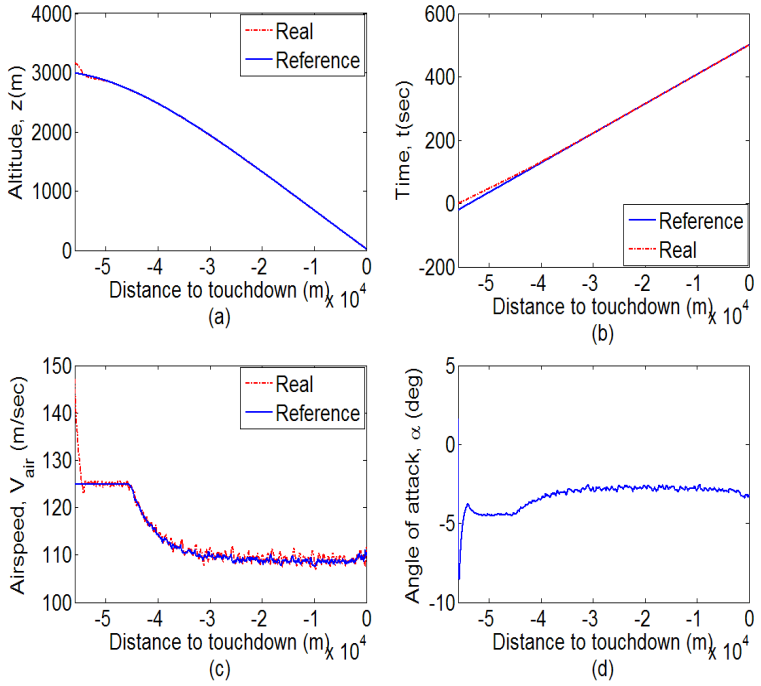

Fig. 10 Delayed initial situation and recover with wind.

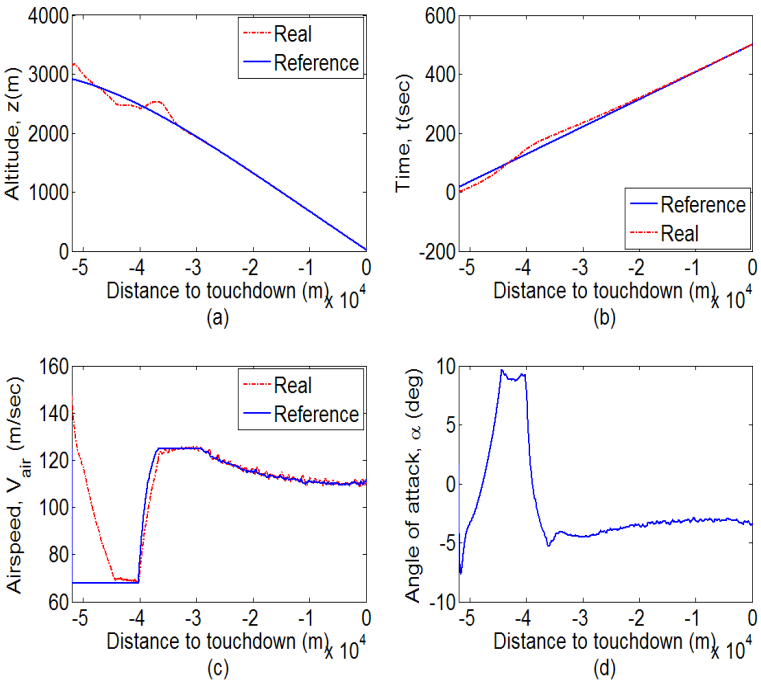

Fig. 11 Advanced initial situation and recover with wind.